Data-driven Wave Feedforward Control of Floating Offshore Wind Turbines

Ministeru, Alexandra; Hegazy, Amr; Van Wingerden, Jan Willem

DOI
10.23919/ACC63710.2025.11108107

Publication date
2025

Document Version
Final published version

Published in
Proceedings of the American Control Conference, ACC 2025

2025 American Control Conference (ACC)
July 8-10, 2025. Denver, CO, USA

Data-driven Wave Feedforward Control of Floating Offshore Wind Turbines

Alexandra Ministeru[1], Amr Hegazy[1] and Jan-Willem van Wingerden[1]

***Abstract*— Floating offshore wind turbines pave the way to accessing deep-water regions with abundant wind resources. However, they face specific control challenges, such as the negative damping problem and increased model complexity. Since model-based control is becoming increasingly demanding, a model-free, data-driven approach is considered. Additionally, floating wind turbines are susceptible to rough environmental disturbances. Feedforward information, such as wave elevation measurements from wave radars, may be included in the controller to lessen the impact of disturbances. Although waves have been shown to increase rotor speed oscillations and turbine loads, wave-preview-based methods have only recently been explored. To this end, this paper first proposes a modified Data-enabled Predictive Control formulation that includes past and future information about measurable disturbances. The feasibility of this control strategy is then demonstrated for floating wind turbines through mid-fidelity simulations. The model-free, feedforward controller uses a preview of wave forces acting on the floating platform and aims for rotor speed regulation. Simulations indicate that the data-driven approach has potential for floating wind turbine control, and including wave feedforward action reduces the amplitude of rotor speed oscillations.**

I. INTRODUCTION

Floating offshore wind turbines (FOWTs) can extract wind energy in deep-sea locations that are not accessible to fixed-bottom offshore wind turbines [1]. However, due to the floating platform and placement in harsh environmental conditions, FOWTs face a distinctive set of control challenges compared to their fixed-bottom counterparts.

In the above-rated operational region, a traditional fixed-bottom wind turbine controller leads to undamped pitching motions of the floater, a phenomenon known as the negative damping problem [2]. In terms of control, a trade-off between rotor speed regulation and platform pitching motion reduction arises [3]. There are numerous attempts at adapting the conventional controller of a fixed-bottom wind turbine to solve the negative damping issue, and model-based, multi-objective methods are largely recommended [4].

Among advanced control methods, the Model Predictive Control (MPC) framework is of particular interest, since it is appropriate for constrained MIMO systems. A well-researched topic for non-floating wind turbines, MPC has also been implemented for floating structures with good results [5]–[7]. Nevertheless, MPC requires a good system model.

Capturing the behavior of a FOWT within a linear time-invariant (LTI) model with a sufficient level of fidelity has proven to be non-trivial. For instance, the increase in rotor size accentuates the nonlinear phenomena [8], while additional rotor motions are introduced by the floating platform [9]. Furthermore, obtaining an accurate model is a challenging process that requires considerable effort and expert knowledge [10]. Thus, circumventing the need for a plant representation during control design is a topic of interest.

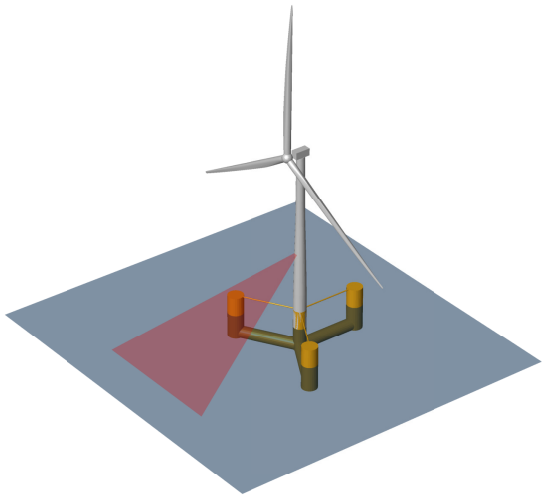

Fig. 1: Concept of an IEA-15MW reference wind turbine mounted on a VolturnUS-S floater with a wave radar installed on the tower. The radar provides upstream water elevation measurements, which can be used for feedforward control.

A considerable amount of data can be collected from wind turbine sensors and leveraged through data-driven control (DDC). Direct DDC methods use input-output data to obtain future control commands without explicitly computing a system realization in the process [11]. Since a model is never used, issues such as model uncertainty, unmodeled dynamics, or model complexity no longer present a limitation [10]. Among direct DDC approaches, Subspace Predictive Control (SPC) [12] and Data-enabled Predictive Control (DeePC) [13] propose frameworks similar to that of MPC, allowing for a constrained optimization criterion applied in a receding horizon manner. These methods can be used in a reference tracking setting, and SPC has been successfully adapted for periodic load mitigation [14]. However, these methods have not been applied to FOWTs.

The authors would like to acknowledge the support by the Dutch National Research Council (NWO) under the research programme Dutch Research Agenda – research along NWA routes by consortia that supports the Hybrid-Labs project (project number NWA.1518.22.066). This work has received support from the FLOATFARM project, funded by the European Union's Horizon research and innovation program (grant no. 101136091).

[1]Delft University of Technology, Delft Center for Systems and Control, Mekelweg 2, 2628 CD Delft, The Netherlands. {A.Ministeru, A.R.Hegazy, J.W.vanWingerden}@tudelft.nl.

A limitation of feedback control is that disturbances can only be counteracted once they have occurred. FOWTs operate in locations with complex aerodynamic and hydrodynamic disturbances, causing stability issues, decreased performance due to oscillations, and higher structural loads compared to non-floating structures [15]. To prevent this, feedforward (FF) action can be included to complement the feedback controller. A measurement of incoming disturbances is necessary for FF control. Among measuring methods, Light Detection and Ranging (LIDAR) systems gained popularity: future wind disturbance is most often employed for feedforward FOWT control [16]–[18]. Regarding data-driven algorithms, LIDAR wind knowledge has been recently integrated with SPC [19]. To mitigate hydrodynamic disturbances, wave radars can be installed on the tower of floating turbines, as illustrated in Fig. 1. Using water elevation measurements, wave excitation forces can be estimated through wave prediction models [20] and incorporated in the wind turbine controller. However, wave FF control has only recently been explored [21], [22], despite the considerable impact of waves on FOWTs [23].

Current formulations of DeePC often approach the challenge of non-measurable process and output noise, while measurable disturbances are not considered. A step in this direction was taken in [24], where a past disturbance measurement was included in the DeePC algorithm, while future disturbances are considered unknown. Therefore, incorporating measurements of past and future disturbances in the theoretical framework of DeePC presents an open opportunity.

Considering all of the above, the contributions of this paper are twofold:

- extend the framework of DeePC with instrumental variables [25] by including a preview of measurable disturbances, therefore opening the possibility of feedforward control.
- explore the feasibility of data-driven wave feedforward control for FOWTs in a mid-fidelity simulation environment to reduce the effect of waves acting on the floating platform.

The remainder of this paper is organized as follows. Section II introduces the modified DeePC framework that includes feedforward knowledge. In Section III, the modified DeePC algorithm is presented. Section IV shows the results of a mid-fidelity simulation with the proposed controller in steady and turbulent wind conditions. Finally, the conclusion is given in Section V.

II. DATA-ENABLED PREDICTIVE CONTROL WITH FUTURE DISTURBANCE

A. Model structure

The extension below follows the derivation in [25]. The underlying process assumed to generate the input-output data sets is a discrete-time LTI system, described by a state-space model in innovation form:

$$x_{k+1} = Ax_k + B_u u_k + B_d d_k + Ke_k, \tag{1a}$$
$$y_k = Cx_k + D_u u_k + D_d d_k + e_k, \tag{1b}$$

where $x_k \in \mathbb{R}^n$, $u_k \in \mathbb{R}^r$, $d_k \in \mathbb{R}^q$, $y_k \in \mathbb{R}^\ell$, represent the state, input, disturbance, and output vectors, respectively. Although the disturbance acts as an input to the plant, it is represented separately from the control input because it is not controllable. The matrices $A, B_u, B_d, K, C, D_u, D_d$ are the system matrices of appropriate dimensions, while $k \in \mathbb{Z}_{\geq 0}$ is the discrete time index. The system is subject to measurement and process noise, $e_k \in \mathbb{R}^\ell$ representing an ergodic white noise signal with zero mean and covariance matrix $\mathbb{W}\{e_j e_k^\top\} = W\delta_{ij}$, with $W \succ 0$. It is assumed that (1) is a controllable system in a minimal realization [13], and $\tilde{A} = A - KC$ has all eigenvalues inside the open unit circle.

By eliminating e_k from (1a), the system can be alternatively represented in the predictor form:

$$x_{k+1} = \tilde{A}x_k + \tilde{B}_u u_k + \tilde{B}_d d_k + Ky_k, \tag{2a}$$
$$y_k = Cx_k + D_u u_k + D_d d_k + e_k, \tag{2b}$$

with $\tilde{A} = A - KC$, $\tilde{B}_u = B_u - KD_u$, $\tilde{B}_d = B_d - KD_d$.

B. Notations and assumptions

Several notations of frequently used matrices will be introduced before proceeding to the derivation of the DeePC framework that includes disturbance knowledge. A block-Hankel matrix is defined as:

$$U_{i,s,\bar{N}} = \begin{bmatrix} u_i & u_{i+1} & \cdots & u_{i+\bar{N}-1} \\ u_{i+1} & u_{i+2} & \cdots & u_{i+\bar{N}} \\ \vdots & \vdots & \ddots & \vdots \\ u_{i+s-1} & u_{i+s} & \cdots & u_{i+\bar{N}+s-2} \end{bmatrix},$$

where $U_{i,s,\bar{N}} \in \mathbb{R}^{rs\times\bar{N}}$, $i \in \mathbb{Z}$, and $\{s, \bar{N}\} \in \mathbb{Z}_{>0}$. For clarity, i indicates the index of the first element of the matrix, s represents the block size, while $\bar{N}$ indicates the number of columns. To construct this block-Hankel matrix, $\bar{N} + s - 1$ data samples are necessary. The block matrices $Y_{i,s,\bar{N}} \in \mathbb{R}^{\ell s\times\bar{N}}$, $E_{i,s,\bar{N}} \in \mathbb{R}^{\ell s\times\bar{N}}$, and $D_{i,s,\bar{N}} \in \mathbb{R}^{qs\times\bar{N}}$ are similarly defined, using output, noise and disturbance data respectively. In the case of block-Hankel matrices with only one block-row ($s = 1$), the second index is omitted. This is the case for state sequences, with $X_{i,\bar{N}} \in \mathbb{R}^{n\times\bar{N}}$:

$$X_{i,\bar{N}} = \begin{bmatrix} x_i & x_{i+1} & \cdots & x_{i+\bar{N}-1} \end{bmatrix}.$$

For a prediction window of length $f \in \mathbb{Z}_{>0}$, block-Toeplitz matrices are defined as

$$H^{(f)}_{(\tilde{B}_u,D_u)} = \begin{bmatrix} D_u & 0 & 0 & \cdots & 0 \\ C\tilde{B}_u & D_u & 0 & \cdots & 0 \\ \vdots & \vdots & \ddots & \ddots & \vdots \\ C\tilde{A}^{f-2}\tilde{B}_u & C\tilde{A}^{f-3}\tilde{B}_u & \cdots & C\tilde{B}_u & D_u \end{bmatrix},$$

where $H^{(f)}_{(\tilde{B}_u,D_u)} \in \mathbb{R}^{\ell f\times rf}$. Similarly, $H^{(f)}_{(\tilde{B}_d,D_d)} \in \mathbb{R}^{\ell f\times qf}$ and $H^{(f)}_{(K,I)} \in \mathbb{R}^{\ell f\times\ell f}$ are defined, where I represents the identity matrix of appropriate size.

With a past window of length $p \in \mathbb{Z}_{>0}$, the extended controllability matrix is defined as

$$\mathcal{K}^{(p)}_{(\tilde{B}_u)} = \begin{bmatrix} \tilde{A}^{p-1}\tilde{B}_u & \tilde{A}^{p-2}\tilde{B}_u & \cdots & \tilde{B}_u \end{bmatrix},$$

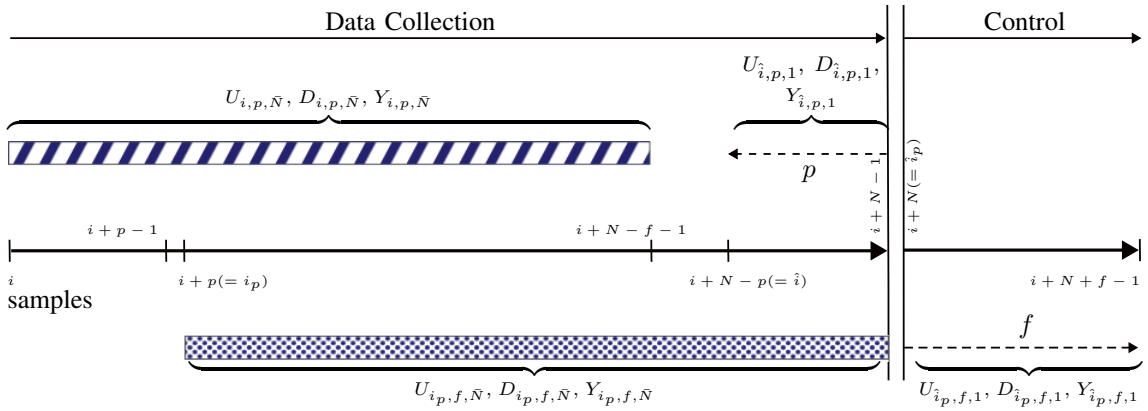

Fig. 2: Partition of the data set used by the DeePC algorithm. The batch gathered during the offline data collection stage is split into two sets and used to derive the characteristic equation. During the online control stage, the last p measurements initialize the optimal controller and enable the prediction of the evolution of the future input-output trajectories over a future horizon of length f. Figure adapted from [25].

with $\mathcal{K}^{(p)}_{(\tilde{B}_u)} \in \mathbb{R}^{n\times rp}$. Additionally, $\mathcal{K}^{(p)}_{(\tilde{B}_d)} \in \mathbb{R}^{n\times qp}$, and $\mathcal{K}^{(p)}_{(K)} \in \mathbb{R}^{n\times \ell p}$ are introduced. For conciseness, the controllability matrices are collected in $\mathcal{K} = \begin{bmatrix}\mathcal{K}^{(p)}_{(\tilde{B}_u)} & \mathcal{K}^{(p)}_{(\tilde{B}_d)} & \mathcal{K}^{(p)}_{(K)}\end{bmatrix} \in \mathbb{R}^{n\times(r+q+\ell)p}$.

The extended observability matrix is given as:

$$\Gamma^{(f)} = \begin{bmatrix} C \\ C\tilde{A} \\ C\tilde{A}^2 \\ \vdots \\ C\tilde{A}^{f-1} \end{bmatrix}, \tag{3}$$

where $\Gamma^{(f)} \in \mathbb{R}^{\ell f\times n}$. The identity matrix is denoted by I, while O and o stand for the zero matrix and vector respectively, all of suitable dimensions. Additionally, a vector of ones is denoted as $\mathbf{1}_n = \begin{bmatrix}1 & 1 & \cdots & 1\end{bmatrix}^\top \in \mathbb{R}^n$.

The following assumptions are used throughout this paper:

Assumption 1. The input, output, and disturbance signals are measurable.

Assumption 2. Both input and disturbance sequences are persistently exciting of order at least $p+f+n$, where n is the order of the minimal representation in (1) [13].

Assumption 3. A disturbance preview of length f is available at any given point during the control stage.

Assumption 4. The signal e_k is a zero-mean white noise, uncorrelated to the input and disturbance signals.

C. The data equation

Synthesizing the DeePC controller requires a data collection stage. The data batch of size N is first partitioned into two overlapping sets, the so-called past and the so-called future, represented in Fig. 2 by the striped and the dotted bar, respectively. The data points from the striped segment are organized in the input $U_{i,p,\bar{N}}$, disturbance $D_{i,p,\bar{N}}$, and output $Y_{i,p,\bar{N}}$ block-Hankel matrices, where $\bar{N} = N-p-f+1$. Similarly, matrices $U_{i_p,f,\bar{N}}$, $D_{i_p,f,\bar{N}}$, and $Y_{i_p,f,\bar{N}}$ are constructed using data from the dotted segment, where $i_p = i+p$.

For the DeePC formulation, a few additional data matrices are necessary. Corresponding to the dashed arrow pointing to the left, the last p input-output samples of the data set are gathered in $U_{\hat{i},p,1}$, $D_{\hat{i},p,1}$, and $Y_{\hat{i},p,1}$, with $\hat{i} = i+N-p$. Starting from $\hat{i}_p = i+N$, the vectors $U_{\hat{i}_p,f,1}$, $D_{\hat{i}_p,f,1}$ and $Y_{\hat{i}_p,f,1}$ are employed. These vectors correspond to the dashed arrow pointing toward the right of the sample axis, which is outside of the collected data set. It is important to note that $U_{\hat{i}_p,f,1}$ and $Y_{\hat{i}_p,f,1}$ contain unknown samples, while $D_{\hat{i}_p,f,1}$ is fully known.

The aim of the disturbance feedforward DeePC is to find an optimal future input command $U_{\hat{i}_p,f,1}$ such that $Y_{\hat{i}_p,f,1}$ follows a prescribed reference r_f in the presence of a known disturbance $D_{\hat{i}_p,f,1}$, based on a connection between the known and unknown data trajectories.

Starting from $k = i_p$ with an initial state x_{i_p}, equation (2) is propagated for $f-1$ steps forward in time and the resulting outputs are concatenated in the vector $y^\top_{i_p,f,1} = \begin{bmatrix}y^\top_{i_p} & y^\top_{i_p+1} & \cdots & y^\top_{i_p+f-1}\end{bmatrix}$. To cover the entire set of so-called future outputs, this process is repeated for a total of $\bar{N}$ times for each time index of the remaining data batch and the resulting vectors are stacked in block-Hankel matrices, compactly described as:

$$\begin{aligned} Y_{i_p,f,\bar{N}} =& \Gamma^{(f)} X_{i_p,\bar{N}} + H^{(f)}_{(\tilde{B}_u,D_u)} U_{i_p,f,\bar{N}} \\ &+ H^{(f)}_{(\tilde{B}_d,D_d)} D_{i_p,f,\bar{N}} + H^{(f)}_{(K,I)} E_{i_p,f,\bar{N}}. \end{aligned} \tag{4}$$

The sequence of initial states $X_{i_p,\bar{N}}$ is, however, unknown. Consequently, $Y_{i_p,f,\bar{N}}$ does not solely rely on measured trajectories. Thus, an approach often encountered in subspace identification is used to express the state in terms of input-output data [26]. A state x_k can be iteratively propagated forward using (2a) over p time samples. The resulting state x_{k+p} will depend only on the initial state x_k and input-output data:

$$x_{k+p} = \tilde{A}^p x_k + \mathcal{K} \begin{bmatrix} U_{k,p,1} \\ D_{k,p,1} \\ Y_{k,p,1} \end{bmatrix}. \tag{5}$$

Since all eigenvalues of $\tilde{A}$ are situated inside the open unit circle, $||\tilde{A}^p||_F$ becomes arbitrarily small if the size of the past window p is large enough. This is a common assumption in subspace identification [27], and it is assumed to hold here as well. The influence of the initial state becomes negligible, and the first term of (5) can be omitted. Introducing this approximation in (4) yields the data equation:

$$\begin{aligned} Y_{i_p,f,\bar{N}} =& \Gamma^{(f)}\mathcal{K}\begin{bmatrix} U_{i,p,\bar{N}} \\ D_{i,p,\bar{N}} \\ Y_{i,p,\bar{N}} \end{bmatrix} + H^{(f)}_{(\tilde{B}_u,D_u)}U_{i_p,f,\bar{N}} \\ &+ H^{(f)}_{(\tilde{B}_d,D_d)}D_{i_p,f,\bar{N}} + H^{(f)}_{(K,I)}E_{i_p,f,\bar{N}}. \end{aligned} \tag{6}$$

This equation only depends on input, output, and disturbance trajectories, along with system matrices, and it is further used to derive the disturbance feedforward DeePC algorithm. Before proceeding to the characteristic equation, a similar relation is given between the past and future data corresponding to the dashed arrows:

$$\begin{aligned} Y_{\hat{i}_p,f,1} =& \Gamma^{(f)}\mathcal{K}\begin{bmatrix} U_{\hat{i},p,1} \\ D_{\hat{i},p,1} \\ Y_{\hat{i},p,1} \end{bmatrix} + H^{(f)}_{(\tilde{B}_u,D_u)}U_{\hat{i}_p,f,1} \\ &+ H^{(f)}_{(\tilde{B}_d,D_d)}D_{\hat{i}_p,f,1} + H^{(f)}_{(K,I)}E_{\hat{i}_p,f,1}. \end{aligned} \tag{7}$$

D. The disturbance DeePC characteristic equation

By manipulation of (6)-(7) as shown in [25], the characteristic equation of DeePC including disturbance knowledge can be obtained. The following illustrates a deterministic case:

$$\begin{bmatrix} \begin{bmatrix} U_{i,p,\bar{N}} \\ D_{i,p,\bar{N}} \\ Y_{i,p,\bar{N}} \end{bmatrix} \\ U_{i_p,f,\bar{N}} \\ D_{i_p,f,\bar{N}} \end{bmatrix} g = \begin{bmatrix} \begin{bmatrix} U_{\hat{i},p,1} \\ D_{\hat{i},p,1} \\ Y_{\hat{i},p,1} \end{bmatrix} \\ U_{\hat{i}_p,f,1} \\ D_{\hat{i}_p,f,1} \end{bmatrix}, \tag{8}$$

$$Y_{i_p,f,\bar{N}}g = Y_{\hat{i}_p,f,1}, \tag{9}$$

where $g \in \mathbb{R}^{\bar{N}\times 1}$. This outlines how future trajectories of the system can be expressed as linear combinations of past input-output trajectories, as long as the input sequence was sufficiently exciting and the left-hand side block matrix has full rank. Equation (9) is split from (8), in accordance with [28]. If the left-hand side data matrix in (8) contains noise-corrupted trajectories, deterministic DeePC does not ensure the feasibility of the predicted future trajectories for the real system [29]. To mitigate the effect of process or measurement noise, an instrumental variable $Z_{\bar{N}}$ is used, similar to [25]. A $Z_{\bar{N}}$ candidate must satisfy two properties [26]. First, the future noise data matrix must be uncorrelated to $Z_{\bar{N}}$, such that when taking the limit for $\bar{N} \to \infty$, its bias is removed:

$$\lim_{\bar{N}\to\infty} \frac{1}{\bar{N}} \left(E_{i_p,f,\bar{N}} Z_{\bar{N}}^\top \right) = O. \tag{10}$$

The second property ensures that introducing the instrumental variable does not change the rank of the data matrix. Thus, the subspace spanned by the trajectories in the data matrix is not reduced:

$$\text{rank}\left(\lim_{\bar{N}\to\infty} \frac{1}{\bar{N}} \begin{bmatrix} U_{i,p,\bar{N}} \\ D_{i,p,\bar{N}} \\ Y_{i,p,\bar{N}} \\ U_{i_p,f,\bar{N}} \\ D_{i_p,f,\bar{N}} \end{bmatrix} Z_{\bar{N}}^\top \right) = \text{rank}\left(\begin{bmatrix} U_{i,p,\bar{N}} \\ D_{i,p,\bar{N}} \\ Y_{i,p,\bar{N}} \\ U_{i_p,f,\bar{N}} \\ D_{i_p,f,\bar{N}} \end{bmatrix} \right). \tag{11}$$

A candidate matrix that satisfies these properties is given below, where $Z_{\bar{N}} \in \mathbb{R}^{(r+q+\ell)p+(r+q)f\times\bar{N}}$:

$$Z_{\bar{N}} = \begin{bmatrix} U_{i,p,\bar{N}} \\ D_{i,p,\bar{N}} \\ Y_{i,p,\bar{N}} \\ U_{i_p,f,\bar{N}} \\ D_{i_p,f,\bar{N}} \end{bmatrix}. \tag{12}$$

Introducing the instrumental variable, $Z_{\bar{N}}^\top$, in (8)-(9) with a vector $\hat{g} \in \mathbb{R}^{(r+q+\ell)p+(r+q)f\times 1}$ results in:

$$\lim_{\bar{N}\to\infty} \left(\begin{bmatrix} \begin{bmatrix} U_{i,p,\bar{N}} \\ D_{i,p,\bar{N}} \\ Y_{i,p,\bar{N}} \end{bmatrix} \\ U_{i_p,f,\bar{N}} \\ D_{i_p,f,\bar{N}} \end{bmatrix} Z_{\bar{N}}^\top \hat{g} \right) = \begin{bmatrix} \begin{bmatrix} U_{\hat{i},p,1} \\ D_{\hat{i},p,1} \\ Y_{\hat{i},p,1} \end{bmatrix} \\ U_{\hat{i}_p,f,1} \\ D_{\hat{i}_p,f,1} \end{bmatrix}, \tag{13}$$

$$\lim_{\bar{N}\to\infty} Y_{i_p,f,\bar{N}} Z_{\bar{N}}^\top \hat{g} = Y_{\hat{i}_p,f,1}. \tag{14}$$

With this formulation, the effect of noise is asymptotically removed. In practice, $\bar{N}$ should be chosen high enough to ensure this property is sufficiently satisfied. Even though this translates to a necessity for a high amount of data points, the introduction of the instrumental variable leads to an important reduction in the size of the DeePC problem: the optimization vector variable $\hat{g}$ decreases from a size of $\bar{N}$ in the deterministic case, to $(r+q+\ell)p+(r+q)f$.

III. DISTURBANCE FEEDFORWARD DEEPC

The behavior of the underlying process is now captured by (13)-(14). The formulation of the DeePC optimization problem extended with disturbance preview follows as:

$$\begin{aligned} \min_{U_{\hat{i}_p,f,1},\hat{g}} \; & (Y_{\hat{i}_p,f,1} - r_f)^\top Q (Y_{\hat{i}_p,f,1} - r_f) + U_{\hat{i}_p,f,1}^\top R U_{\hat{i}_p,f,1} \\ \text{s.t.} \; & \begin{bmatrix} U_{i,p,\bar{N}} \\ D_{i,p,\bar{N}} \\ Y_{i,p,\bar{N}} \\ U_{i_p,f,\bar{N}} \\ D_{i_p,f,\bar{N}} \end{bmatrix} Z_{\bar{N}}^\top \hat{g} = \begin{bmatrix} U_{\hat{i},p,1} \\ D_{\hat{i},p,1} \\ Y_{\hat{i},p,1} \\ U_{\hat{i}_p,f,1} \\ D_{\hat{i}_p,f,1} \end{bmatrix}, \\ & Y_{i_p,f,\bar{N}} Z_{\bar{N}}^\top \hat{g} = Y_{\hat{i}_p,f,1}, \\ & u_k \in \mathcal{U}, \forall k \in \{0,\cdots,f-1\}, \\ & y_k \in \mathcal{Y}, \forall k \in \{0,\cdots,f-1\}, \end{aligned} \tag{15}$$

where $Q \in \mathbb{R}^{\ell f\times\ell f}$, $Q \succeq 0$, and $R \in \mathbb{R}^{rf\times rf}$, $R \succ 0$ are the output and input block diagonal weight matrices, respectively. The reference over the future horizon is given by $r_f \in \mathbb{R}^{\ell f}$. $\mathcal{U} \in \mathbb{R}^r$ and $\mathcal{Y} \in \mathbb{R}^\ell$ are the sets of admissible inputs and

outputs, while u_k and y_k represent a shorthand notation for any element of the unknown future input and output vectors, $U_{\hat{i}_p,f,1}$ and $Y_{\hat{i}_p,f,1}$, respectively. It is assumed that the length of the data set N is large enough such that the limit notation in (13)-(14) can be omitted. After the data collection stage is complete and control is activated, the optimal control input is found by solving this optimization problem in a receding horizon manner at each time step and applying only the first element of the sequence to the system. The first part of the cost function penalizes the reference tracking error or corresponds to the disturbance rejection scenario if the reference is constant. Large amplitudes of the control input are prevented through the second part of the objective function. The algorithm of disturbance DeePC is given in Algorithm 1.

Algorithm 1 Disturbance DeePC

Require: N I/O data points $\{u_k, d_k, y_k\}_{k=0}^{N-1}$, a reference trajectory $r_f \in \mathbb{R}^{\ell f}$, past trajectories $U_{-p,p,1}$, $D_{-p,p,1}$, $Y_{-p,p,1}$, the constraint sets $\mathcal{U}$ and $\mathcal{Y}$, and the weight matrices Q and R.

1: At time t, get the disturbance preview $D_{t,f,1}$ and solve (15).
2: Apply the input $U^*_{t,f,1}(t)$.
3: Set $t \leftarrow t+1$ and update $U_{t-p,p,1}, D_{t-p,p,1}, Y_{t-p,p,1}$ to the most recent p I/O measurements.
4: Go back to 1.

IV. FLOATING OFFSHORE WIND TURBINE SIMULATION

The disturbance DeePC formulation proposed in the previous section is applied for FOWT control. The model-free controller is subjected to mid-fidelity simulations using QBLADE, a modular implementation of highly efficient multi-fidelity aerodynamic, structural dynamic, and hydrodynamic solvers [30]. With a software-in-loop interface, QBLADE enables controlling the simulation loop while co-simulating from MATLAB. The NREL 5-MW reference wind turbine [31] mounted on the OC3-Hywind spar-buoy concept platform [32] is employed.

A. Controller configuration

The collective blade pitch angle is used as a controllable input, and the controller objective is reference tracking of the rotor speed. Platform motion reduction is not directly targeted, as using blade pitch control for platform motion reduction proved ineffective [33]. However, the platform pitch angle is restricted through hard constraints. The wave pitching moment acting on the floating platform is considered as the previewed disturbance, while the absolute horizontal wind speed at the rotor acts as a non-controllable, non-previewed (disturbance) input. The control block scheme is illustrated in Fig. 3. Detrending and scaling of the input-output and disturbance signals were adopted to ensure numerical stability during optimization and uniform priority of the signals during control.

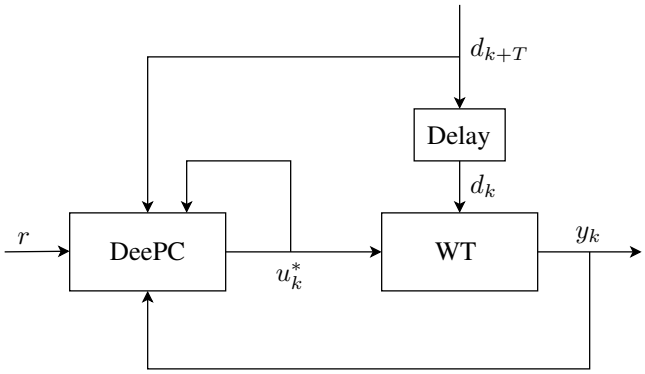

Fig. 3: Block-diagram of the DeePC controller. The DeePC algorithm completely replaces the feedback baseline controller of the wind turbine. The controller relies on output measurements y_k to compute the optimal input u_k^*. Simultaneously, knowledge of future perturbations d_{k+T} is incorporated in the optimization. Thus, the DeePC block combines feedback and feedforward action in one input.

B. Simulation set-up

Simulations are carried out at an operating point corresponding to a mean horizontal wind speed of $16\,\mathrm{m\,s^{-1}}$. The mean wind speed remains constant throughout the simulations. In line with *Assumption 3* of Section II, a preview of the wave pitch moment is available at every point during the simulation. Obtaining such a wave forecast in a real setting is feasible using wave radar technology already developed in the maritime sector.

Two simulation cases are considered. First, the controller is tested in steady wind and irregular wave conditions to outline the effect of including a wave preview in the controller. Second, an irregular wave, turbulent wind inflow scenario with a turbulence intensity of 5% is evaluated for more realistic operating conditions. To generate irregular waves, a JONSWAP spectrum is used, with a significant wave height of $3\,\mathrm{m}$ and a peak spectral period of $12\,\mathrm{s}$. The waves are unidirectional, with a heading direction of 0°. The spectrum of the waves predominantly lies in between $0.05\,\mathrm{Hz}$ and $0.3\,\mathrm{Hz}$, and only normal sea states are considered.

The proposed FF controller's performance is compared to a detuned version of the fixed-bottom baseline controller [32]. The gains of the PI controller are detuned, or lowered, to lessen the negative damping problem, an issue caused by a pair of right-half plane zeros that limit the bandwidth of the blade pitch controller [34]. Increasing the controller's gain causes the closed-loop poles to migrate toward the open-loop zeros, eventually leading to instability. In contrast, decreasing the gains reduces the bandwidth of the blade pitch controller, such that the controller does not excite the platform pitching natural frequency. This results in a platform pitching motion reduction at the cost of increased rotor speed and power oscillations [2]. Additionally, a DeePC controller without knowledge of past and future disturbances is evaluated.

C. Open-loop data collection

During the data collection stage, the system is persistently excited with a pseudo-random binary sequence of blade pitch angle commands with an amplitude of 2°. Even though pitch actuator dynamics are not explicitly considered, every pitch command is maintained for at least $5\,\mathrm{s}$ to allow a realistic interval for pitch actuators to reach the reference value. Irregular waves are allowed to act on the system, along with a zero-mean white noise horizontal wind speed sequence with a variance of $0.25\,\mathrm{m}^2/\mathrm{s}^2$. The input-output trajectories are recorded after the wind turbine has reached a steady state. Data collection is performed only once, before control is initiated, and the data matrices are not subsequently updated.

D. Parameter tuning

For meaningful wave-based feedforward control, a full period of a wave should be included in the preview. However, the slowest considered wave has a period of approximately $20\,\mathrm{s}$. To maintain a reasonable dimension of the optimization problem while capturing enough information in the wave preview, the controller uses a sampling time $T_s = 1\,\mathrm{s}$. The simulation has a shorter sampling time of $0.05\,\mathrm{s}$. The control signal is, therefore, upsampled to 20Hz through a zero-order hold and then low-pass filtered at $1\,\mathrm{Hz}$ to eliminate the high-frequency content introduced by the zero-order hold reconstruction.

The number of decision variables and constraints of the optimization problem is directly proportional to the amount of samples in the past and future windows, p and f. The future window has a length of $f = 20$ samples, equivalent to $20\,\mathrm{s}$. The length of the disturbance preview is equal to the prediction horizon f of the DeePC problem. A shorter preview window proved insufficient for wave effect mitigation, and larger values did not significantly improve performance. A past window $p = 20$ is used in steady wind conditions, whereas for turbulent wind, $p = 40$ was chosen. The length of the data window is selected as $N = 500$. The optimization weights Q and R were tuned to balance the control objective and excessive actuator use penalization.

E. Constraints

Due to physical restrictions, the collective blade pitch angle requires a lower and an upper bound. To prevent destabilization of the turbine, the platform pitch angle is restrained as well. Therefore, for the defined FOWT control problem, the sets $\mathcal{U}$ and $\mathcal{Y}$ in (15) can be generally described as:

$$\begin{aligned} u_{min} \leq u_k \leq u_{max}, \forall k \in \{0, \cdots, f-1\}, \\ y_{min} \leq y_k \leq y_{max}, \forall k \in \{0, \cdots, f-1\}. \end{aligned} \tag{16}$$

Moreover, the wind turbine's blade pitch actuators have pitching speed limitations. The rate of change of the control input command must also be constrained:

$$|\dot{u}_k| \leq \dot{u}_{max}, \forall k \in \{0, \cdots, f-1\}. \tag{17}$$

This can be rewritten as a set of linear inequations:

$$\begin{aligned} TU_{\hat{i}_p,f,1} \leq \bar{u}_{max} \otimes \mathbf{1}_{r(f-1)} + T_0 U_{\hat{i},p,1}, \\ T = \begin{bmatrix} I & 0 & \cdots & 0 \\ -I & I & \cdots & 0 \\ \vdots & \ddots & \ddots & \vdots \\ 0 & \cdots & -I & I \end{bmatrix}, T_0 = \begin{bmatrix} 0 & 0 & \cdots & I \\ 0 & 0 & \cdots & 0 \\ \vdots & \ddots & \ddots & \vdots \\ 0 & 0 & \cdots & 0 \end{bmatrix}, \end{aligned} \tag{18}$$

where $\bar{u}_{max}$ symbolizes the input rate bound $\dot{u}_{max}$ adjusted to the sampling time of the discrete system, and $\otimes$ is the Kronecker product. The term $T_0 U_{\hat{i},p,1}$ does not depend on the optimization variables and is included to account for the initial condition of the blade pitch command.

F. Quadratic programming formulation

The cost function of the disturbance DeePC in (15) can be cast as a quadratic objective:

$$\begin{aligned} \min_x \quad & \frac{1}{2} x^\top H x + c^\top x, \\ H = & \begin{bmatrix} Z_{\bar{N}} Y_{i_p,f,\bar{N}}^\top Q Y_{i_p,f,\bar{N}} Z_{\bar{N}}^\top & 0 \\ 0 & R \end{bmatrix}, \\ c^\top = & \begin{bmatrix} -2 r_f^\top Q Y_{i_p,f,\bar{N}} Z_{\bar{N}}^\top & 0 \end{bmatrix}, \end{aligned} \tag{19}$$

where $x^\top = \begin{bmatrix} \hat{g}^\top & U_{\hat{i}_p,f,1}^\top \end{bmatrix}$. With this formulation and the linear sets of equality and inequality constraints, the optimization can be approached as a quadratic programming problem.

Due to the accentuated nonlinearity of the plant, regularization terms are included to relax the equality constraints in (15) such that an optimum may be found even if the equalities are not strictly satisfied, as described in [28]. Regularization terms were added on the disturbance input and output trajectories, as well as for $\hat{g}$. The regularization weights are chosen to be high enough such that the slack variables are non-zero only if the problem is infeasible, and a 2-norm of the slack variable vectors is used to preserve the convexity of the optimization problem.

G. Simulation results

Results of the baseline controller simulation, the DeePC with no disturbance information, and the DeePC with feedforward knowledge (FF DeePC) in the steady wind scenario are illustrated in Fig. 4. Both data-driven controllers perform rotor speed tracking and reduce the amplitude of the rotor speed oscillations compared to the baseline controller. The FF DeePC leads to the most significant oscillation reduction without incurring larger platform motions than the DeePC without preview.

Incorporating wave feedforward knowledge in the DeePC algorithm leads to increased actuation compared to both the baseline controller and the simple DeePC. A similar outcome was observed with the wave FF model-based approach in [35]. As confirmed in [33], wave feedforward control is not trivial, and including wave preview does not entirely cancel out the rotor speed oscillations.[1]

[1]The effect of wind disturbance was completely canceled out through LIDAR feedforward control in [19] in linear wind turbine simulations.

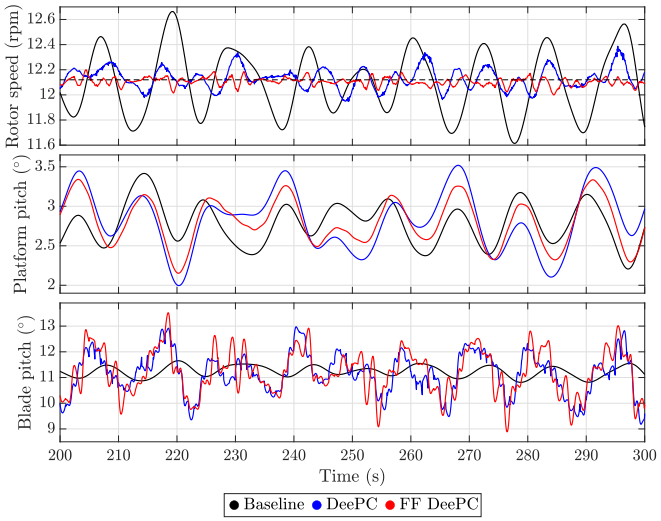

Fig. 4: Part of a mid-fidelity simulation in steady wind and irregular wave conditions. The rotor speed, platform pitch angle, and blade pitch angle input are illustrated. The reference rotor speed is represented as a dashed line in the upper plot.

In Fig. 5, the power spectral density of the signals in Fig. 4 is illustrated. Both data-driven controllers lower the energy carried from the waves to rotor speed oscillations compared to the baseline, with the largest decrease observed for the FF DeePC. Additionally, the DeePC with future knowledge visibly attenuates the energy at the floater's natural pitching frequency, thus lessening the negative damping problem. More energy is condensed in the blade pitch command of the DeePC controllers in the wave frequency range, suggesting that they actively attempt to counteract wave disturbances. The simple DeePC controller is notably exciting in the proximity of the platform pitching eigenfrequency, reflected in both the platform pitch angle and the rotor speed. However, this effect is significantly reduced by introducing wave knowledge in the controller.

Results illustrating the performance of the three controllers in turbulent wind conditions are displayed in Fig. 6. Similarly to the steady wind scenario, the data-driven controllers lower the amplitude of the rotor speed oscillations compared to the baseline. The FF DeePC maintains the rotor speed closer to the reference at the cost of increased blade pitch actuation. To avoid destabilization in turbulent conditions, the pitch angle of the platform is constrained during the optimization and largely remains within the prescribed bounds with both data-driven controllers. The constraint violations are caused by prediction errors. The DeePC algorithm assumes that the underlying system is linear, while the wind turbine model used for simulation is nonlinear. Although the output prediction remains within bounds during the optimization, the actual output may exceed the limits.[2] Additionally, the profile of the wind disturbance is visible at the rotor speed output since the controller is unaware of future wind disturbances. As outlined in [33], above the rated wind speed, the wind is the dominant disturbance, and wave feedforward control becomes difficult.

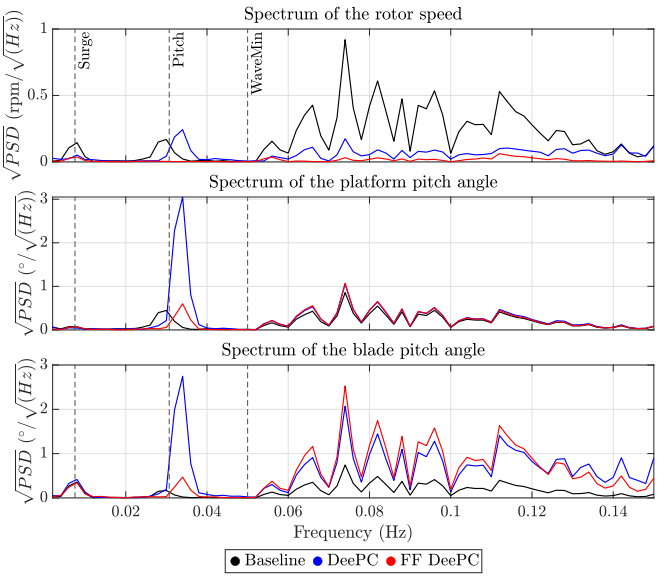

Fig. 5: Square root of the power spectral density of the respective signals in Fig. 4. The platform surge and pitch natural frequencies are marked by the first two vertical dashed lines, respectively. The next vertical line indicates the beginning of the frequency range where the wave disturbance is usually active.

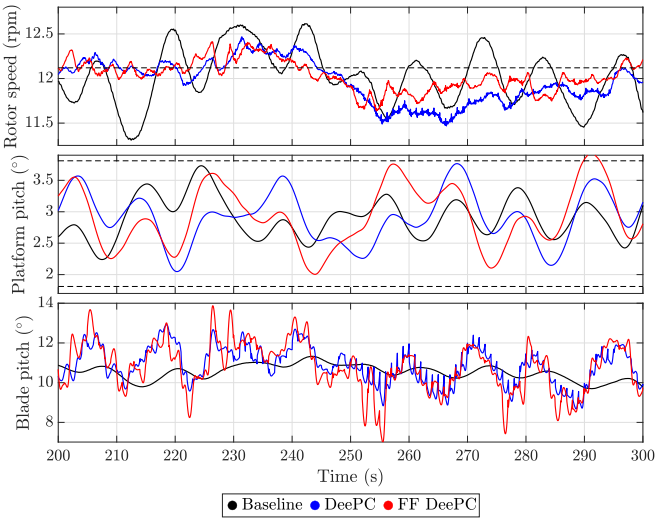

Fig. 6: Part of a mid-fidelity simulation in turbulent wind and irregular wave conditions. The reference rotor speed is represented as a dashed line in the upper plot. The horizontal dashed lines in the middle plot represent constraints used during the optimization.

[2]To guarantee robust output constraint satisfaction, additional considerations would be necessary [36].

V. CONCLUSIONS

In this paper, a DeePC adaptation that enables feedforward control is presented. The algorithm considers past and future information about measurable disturbances to find an optimal control input that compensates for incoming disturbances before they affect the plant. The proposed framework is successfully applied to control a mid-fidelity NREL 5-MW floating offshore wind turbine system. The data-driven controller regulates the rotor speed, and including wave preview in the DeePC controller further reduces the rotor speed oscillations. An attenuation in the platform pitching natural frequency is observed, indicating that DeePC can successfully mitigate the negative damping problem of FOWTs.

REFERENCES

[1] W. Musial, S. Butterfield, and B. Ram, "Energy from offshore wind," in *Offshore technology conference*. OnePetro, 2006.

[2] J. Jonkman, "Influence of control on the pitch damping of a floating wind turbine," in *46th AIAA Aerospace Sciences Meeting and Exhibit*. American Institute of Aeronautics and Astronautics, 2008.

[3] H. Namik and K. Stol, "A review of floating wind turbine controllers," *Handbook of Wind Power Systems*, pp. 415–441, 2013.

[4] F. Lemmer, D. Schlipf, and P. W. Cheng, "Control design methods for floating wind turbines for optimal disturbance rejection," in *Journal of Physics: Conference Series*, vol. 753, no. 9. IOP Publishing, 2016.

[5] K. A. Shah, Y. Li, R. Nagamune, Y. Zhou, and W. U. Rehman, "Platform motion minimization using model predictive control of a floating offshore wind turbine," *Theoretical and Applied Mechanics Letters*, vol. 11, no. 5, 2021.

[6] F. Lemmer, S. Raach, D. Schlipf, and P. W. Cheng, "Prospects of Linear Model Predictive Control on a 10 MW Floating Wind Turbine," in *Volume 9: Ocean Renewable Energy*. St. John's, Newfoundland, Canada: American Society of Mechanical Engineers, 2015, p. V009T09A071.

[7] S. Christiansen, S. M. Tabatabaeipour, T. Bak, and T. Knudsen, "Wave disturbance reduction of a floating wind turbine using a reference model-based predictive control," in *2013 American Control Conference*. IEEE, 2013, pp. 2214–2219.

[8] G. Van Kuik, J. Peinke, R. Nijssen, D. Lekou, J. Mann, J. N. Sørensen, C. Ferreira, J.-W. van Wingerden, D. Schlipf, P. Gebraad *et al.*, "Long-term research challenges in wind energy - a research agenda by the European Academy of Wind Energy," *Wind energy science*, vol. 1, no. 1, pp. 1–39, 2016.

[9] D. Micallef and A. Rezaeiha, "Floating offshore wind turbine aerodynamics: Trends and future challenges," *Renewable and Sustainable Energy Reviews*, vol. 152, p. 111696, Dec. 2021.

[10] Z.-S. Hou and Z. Wang, "From model-based control to data-driven control: Survey, classification and perspective," *Information Sciences*, vol. 235, pp. 3–35, 2013.

[11] F. Dörfler, J. Coulson, and I. Markovsky, "Bridging direct and indirect data-driven control formulations via regularizations and relaxations," *IEEE Transactions on Automatic Control*, vol. 68, no. 2, pp. 883–897, 2022.

[12] W. Favoreel, B. De Moor, and M. Gevers, "SPC: Subspace predictive control," *IFAC Proceedings Volumes*, vol. 32, no. 2, pp. 4004–4009, 1999.

[13] J. Coulson, J. Lygeros, and F. Dörfler, "Data-enabled predictive control: In the shallows of the DeePC," in *2019 18th European Control Conference (ECC)*. IEEE, 2019, pp. 307–312.

[14] Y. Liu, R. M. Ferrari, and J.-W. van Wingerden, "Periodic Load Rejection for Floating Offshore Wind Turbines via Constrained Subspace Predictive Repetitive Control," in *2021 American Control Conference (ACC)*. IEEE, 2021, pp. 539–544.

[15] J. Jonkman and D. Matha, "Dynamics of offshore floating wind turbines—analysis of three concepts," *Wind Energy*, vol. 14, no. 4, pp. 557–569, 2011.

[16] D. Schlipf, E. Simley, F. Lemmer, L. Pao, and P. W. Cheng, "Collective pitch feedforward control of floating wind turbines using lidar," in *The Twenty-fifth International Ocean and Polar Engineering Conference*. OnePetro, 2015.

[17] D. Schlipf, F. Lemmer, and S. Raach, "Multi-variable feedforward control for floating wind turbines using lidar," in *The 30th International Ocean and Polar Engineering Conference*. OnePetro, 2020, p. 340.

[18] T. Wakui, K. Tanaka, and R. Yokoyama, "Reduction in platform motion and dynamic loads of a floating offshore wind turbine-generator system by feedforward control using wind speed preview," *Mechanical Engineering Journal*, vol. 9, no. 4, pp. 1–17, 2022.

[19] R. Dinkla, T. Oomen, J.-W. van Wingerden, and S. P. Mulders, "Data-Driven LIDAR Feedforward Predictive Wind Turbine Control," in *2023 IEEE Conference on Control Technology and Applications (CCTA)*. IEEE, 2023, pp. 559–565.

[20] Y. Ma, P. D. Sclavounos, J. Cross-Whiter, and D. Arora, "Wave forecast and its application to the optimal control of offshore floating wind turbine for load mitigation," *Renewable Energy*, vol. 128, pp. 163–176, 2018.

[21] T. Wakui, A. Nagamura, and R. Yokoyama, "Stabilization of power output and platform motion of a floating offshore wind turbine-generator system using model predictive control based on previewed disturbances," *Renewable Energy*, vol. 173, pp. 105–127, 2021.

[22] A. Hegazy, P. Naaijen, and J.-W. van Wingerden, "Wave feedforward control for large floating wind turbines," in *2023 IEEE Conference on Control Technology and Applications (CCTA)*. IEEE, 2023, pp. 593–598.

[23] M. Al, "Feedforward control for wave disturbance rejection on floating offshore wind turbines," Master's thesis, Delft University of Technology, the Netherlands, 2020.

[24] J. Wang, Y. Zheng, K. Li, and Q. Xu, "DeeP-LCC: Data-enabled predictive leading cruise control in mixed traffic flow," *IEEE Transactions on Control Systems Technology*, 2023.

[25] J.-W. van Wingerden, S. P. Mulders, R. Dinkla, T. Oomen, and M. Verhaegen, "Data-enabled predictive control with instrumental variables: the direct equivalence with subspace predictive control," in *2022 IEEE 61st Conference on Decision and Control (CDC)*. IEEE, 2022, pp. 2111–2116.

[26] M. Verhaegen and V. Verdult, *Filtering and system identification: a least squares approach*. Cambridge University Press, 2007.

[27] G. van der Veen, J.-W. van Wingerden, M. Bergamasco, M. Lovera, and M. Verhaegen, "Closed-loop subspace identification methods: an overview," *IET Control Theory & Applications*, vol. 7, no. 10, pp. 1339–1358, 2013.

[28] J. Coulson, J. Lygeros, and F. Dörfler, "Distributionally robust chance constrained data-enabled predictive control," *IEEE Transactions on Automatic Control*, vol. 67, no. 7, pp. 3289–3304, 2021.

[29] I. Markovsky, L. Huang, and F. Dörfler, "Data-driven control based on the behavioral approach: From theory to applications in power systems," *IEEE Control Systems Magazine*, vol. 43, no. 5, pp. 28–68, 2023.

[30] D. Marten, "QBlade: a modern tool for the aeroelastic simulation of wind turbines," Ph.D. dissertation, Technische Universität Berlin, 2020.

[31] J. Jonkman, S. Butterfield, W. Musial, and G. Scott, "Definition of a 5-MW reference wind turbine for offshore system development," National Renewable Energy Lab. (NREL), Golden, CO (United States), Tech. Rep., 2009.

[32] J. Jonkman, "Definition of the Floating System for Phase IV of OC3," National Renewable Energy Lab. (NREL), Golden, CO (United States), Tech. Rep., 2010.

[33] A. Hegazy, P. Naaijen, V. Leroy, F. Bonnefoy, M. R. Mojallizadeh, Y. Pérignon, and J.-W. van Wingerden, "The potential of wave feedforward control for floating wind turbines: a wave tank experiment," *Wind Energy Science*, vol. 9, no. 8, pp. 1669–1688, 2024.

[34] S. Skogestad and I. Postlethwaite, *Multivariable feedback control: analysis and design*. John Wiley & Sons, 2005.

[35] A. Fontanella, M. Al, J.-W. van Wingerden, and M. Belloli, "Model-based design of a wave-feedforward control strategy in floating wind turbines," *Wind Energy Science*, vol. 6, no. 3, pp. 885–901, 2021.

[36] J. Berberich, J. Köhler, M. A. Müller, and F. Allgöwer, "Robust constraint satisfaction in data-driven MPC," in *2020 59th IEEE Conference on Decision and Control (CDC)*, 2020, pp. 1260–1267.